THE JOURNAL OF PHYSICAL CHEMISTRY A
A JOURNAL OF THE AMERICAN CHEMICAL SOCIETY

pubs.acs.org/JPCA

Article

General Classification of Qubit Encodings in Ultracold Diatomic Molecules

Published as part of The Journal of Physical Chemistry virtual special issue "Physical Chemistry of Quantum Information Science".

Kasra Asnaashari, Roman V. Krems, and Timur V. Tscherbul*

Cite This: *J. Phys. Chem. A* 2023, 127, 6593–6602

Read Online

ACCESS | Metrics & More | Article Recommendations

ABSTRACT: Owing to their rich internal structure and significant long-range interactions, ultracold molecules have been widely explored as carriers of quantum information. Several different schemes for encoding qubits into molecular states, both bare and field-dressed, have been proposed. At the same time, the rich internal structure of molecules leaves many unexplored possibilities for qubit encodings. We show that all molecular qubit encodings can be classified into four classes by the type of the effective interaction between the qubits. In the case of polar molecules, the four classes are determined by the relative magnitudes of matrix elements of the dipole moment operator in the single-molecule basis. We exemplify our classification scheme by considering the encoding of the effective spin-1/2 system into nonadjacent rotational states (e.g., $N = 0$ and 2) of polar and nonpolar molecules with the same nuclear spin projection. Our classification scheme is designed to inform the optimal choice of molecular qubit encoding for quantum information storage and processing applications, as well as for dynamical generation of many-body entangled states and for quantum annealing.

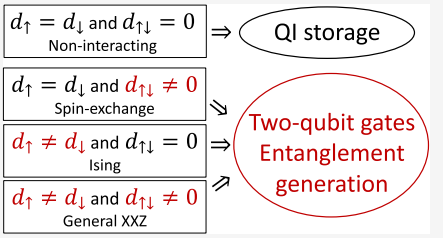

1. INTRODUCTION

Recent experimental progress toward the high-fidelity quantum control of ultracold molecules trapped in optical lattices[1] and tweezers[2] has stimulated much interest in using ultracold molecular gases for quantum information science (QIS) applications. The key advantage offered by ultracold molecules lies in their numerous and diverse degrees of freedom, which include not only electronic and hyperfine states (which are also present in atoms), but also vibrational and rotational modes, all of which could be used to encode a qubit. Additionally, these degrees of freedom allow one to encode quantum information into higher-dimensional Hilbert spaces, which could be used either for high-dimensional quantum computing[3] or quantum error correction.[4] Another crucial advantage of ultracold polar molecules for QIS is afforded by their strong, anisotropic, and tunable electric dipolar (ED) interactions, which can be used to engineer quantum logic gates[5−7] and to generate many-body entangled states.[8−12] Very recently, two-qubit gates between trapped polar molecules were demonstrated experimentally[11,12] via spin-exchange of CaF molecules in optical tweezers.

Several types of molecular qubit encodings have been proposed, including into adjacent rotational states ($N = 0$ and 1) of the same nuclear/electron spin projection,[5,6] nuclear/electron spin sublevels of a single ($N = 0$) rotational state,[6,13−16] nuclear/electron spin sublevels of adjacent rotational states ($N = 0$ and 1),[10] and vibrational states.[17,18] Robust QI storage is favored by qubits that are not affected by the long-range ED interaction,[13,14] whereas high-fidelity QI processing (via two-qubit quantum gates) is easier to achieve with strongly interacting qubits.[6,7] The ability to switch between encodings yielding noninteracting and interacting qubits by means of, e.g., microwave pulses[19,20] is a key component of QIS protocols based on ultracold molecules.[7] This motivates the ongoing search of new qubit encoding schemes. At the same time, the discovery of new qubit encodings may give rise to novel applications of ultracold molecules for quantum computing, such as quantum annealing based on molecules.[21]

Despite the recent proposals,[6,7,10,14−18,21] there remains a wealth of possibilities for unexplored encodings of qubits into molecular states. For example, qubits can be encoded into nonadjacent rotational levels (e.g., $N = 0$ and 2) of the same or different vibronic states, into hyperfine-Zeeman sublevels of the rovibronic states or even into different rovibrational and hyperfine states in different electronic manifolds. This gives rise to the following question: What are the advantages and

Received: April 30, 2023
Revised: June 23, 2023
Published: July 26, 2023

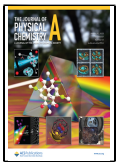

https://doi.org/10.1021/acs.jpca.3c02835
J. Phys. Chem. A 2023, 127, 6593−6602

limitations of a given molecular qubit encoding for QI storage and processing? This question is relevant because, as mentioned, QI storage and processing impose conflicting requirements on the type of encoding. Specifically, good memory qubits must be well-isolated from an external environment, and their interactions with each other must be minimized to avoid decoherence.[22] By contrast, good qubits for processing quantum information must be strongly interacting, with the interactions controllable by external electromagnetic fields.[23]

Motivated by this question, we propose a classification of molecular qubit encodings based on the ED interaction between the qubits. We show that, given the matrix elements of the dipole moment operator in the single-molecule basis, it is possible to assess the potential utility of any given molecular qubit for QI storage and processing applications. As an example, in Section 3, we explore molecular qubit encoding into nonadjacent rotational states (N = 0 and 2), which gives rise to several types of encoding according to our classification scheme. The encodings into the N = 0, 2 and 0, 3 rotational states were briefly mentioned by Gorshkov and co-workers[24] in the context of minimizing tensor ac Stark shifts of trapped molecules. However, to our knowledge, neither single-molecule matrix elements of the electric dipole moment nor the effective ED interactions between the molecules have been explored in the nonadjacent rotational state encoding.

In Section 4, we show that similar arguments can be made for higher-order long-range couplings by considering electric quadrupole and magnetic dipole−dipole interactions. The former are essential for qubit encodings in nonpolar homonuclear molecules. Section 5 concludes with a brief summary of our main results and discusses several directions for future work.

2. CLASSIFICATION OF MOLECULAR QUBIT ENCODINGS

We consider an effective spin-1/2 system with the eigenstates $|\downarrow\rangle$ and $|\uparrow\rangle$ comprising a qubit. A particular encoding identifies $|\downarrow\rangle$ and $|\uparrow\rangle$ with the physical states of a diatomic molecule, such as electronic, vibrational, rotational, fine, hyperfine, Stark, or Zeeman states. The two-qubit and many-qubit Hamiltonians inherit the properties of the molecular states used for the encoding.

As the strong, anisotropic, and tunable electric dipole−dipole (ED) interaction between molecular qubits is central to their applications in QIS,[1,25] we use the ED interaction as a basis of our classification. The effective ED interaction between two isolated spin-1/2 systems encoded in molecules i and j takes the form of the XXZ Hamiltonian[25,26] (see Appendix A for a derivation)

$$\hat{H}_{ij} = \frac{1 - 3\cos^2\theta_{ij}}{R_{ij}^3}\left[\frac{J_\perp}{2}(\hat{S}_i^+\hat{S}_j^- + \text{h.c.}) + J_z\hat{S}_i^z\hat{S}_j^z + W(\hat{I}_i\hat{S}_j^z + \hat{S}_i^z\hat{I}_j) + V\hat{I}_i\hat{I}_j\right] \quad (1)$$

where $\hat{S}_i^\alpha$ and $\hat{S}_j^\alpha$ are the effective spin operators acting in the two-dimensional Hilbert spaces of the ith and jth molecules ($\alpha = \pm, z$), respectively, R_{ij} is the distance between the molecules, and θ_{ij} is the angle between the quantization vector and the vector connecting the two molecules.

To derive eq 1, we assume that the ED interaction between molecules is much weaker than the energy difference between $|\uparrow\rangle$ and $|\downarrow\rangle$. This is a realistic assumption for most molecules trapped in optical lattices and tweezers, for which $|R_{ij}| \geq 500$ nm, and the ED interaction rarely exceeds 1 kHz. As a result, couplings that change the total angular momentum projection of two molecules give rise to energetically off-resonant transitions and can be neglected.[25] Examples of such processes include transitions, which transfer angular momentum from molecular rotation to their relative (orbital) motion ($q = \pm 1$ and $q = \pm 2$, see Appendix A). We further assume that the qubit states $|\uparrow\rangle$ and $|\downarrow\rangle$ are isolated, whether by symmetry or by energy detuning, from other molecular states. This is an essential requirement for any QIS protocol.

As shown in previous work (see, e.g., refs 25, 26) and detailed in Appendix A for the present discussion, the coupling constants in the effective spin−spin interaction Hamiltonian (1)

$$J_z = (d_\uparrow - d_\downarrow)^2 \quad (2)$$

$$J_\perp = 2d_{\uparrow\downarrow}^2 - |d_{\uparrow\downarrow}^+|^2 - |d_{\uparrow\downarrow}^-|^2 \quad (3)$$

can be expressed in terms of the matrix elements of the electric dipole moments (EDMs) of the individual molecules with the spherical tensor components $\hat{d}_p$ ($\hat{d}_0 = \hat{d}_z$, $\hat{d}_{\pm 1} = \mp(\hat{d}_x \pm i\hat{d}_y)/\sqrt{2}$)

$$\langle \uparrow |\hat{d}_0| \uparrow \rangle \equiv d_\uparrow, \quad \langle \downarrow |\hat{d}_0| \downarrow \rangle \equiv d_\downarrow \quad (4)$$

$$\langle \uparrow |\hat{d}_0| \downarrow \rangle \equiv d_{\uparrow\downarrow}, \quad \langle \uparrow |\hat{d}_{\pm 1}| \downarrow \rangle \equiv d_{\uparrow\downarrow}^\pm \quad (5)$$

Significantly, the Ising coupling constant J_z depends on the difference between the diagonal matrix elements of the EDM in the qubit basis, and the spin-exchange coupling $J_\perp$ scales with the square of the off-diagonal (or transition) matrix element. In practice, in the absence of mixing between angular momentum projection states, either $d_{\uparrow\downarrow}$ or $d_{\uparrow\downarrow}^\pm$ vanishes, so either the first or the last two terms on the right-hand side of eq 3 are different from zero. The terms parameterized by the constants $W = (d_\uparrow^2 - d_\downarrow^2)/2$ and $V = (d_\uparrow + d_\downarrow)^2/4$ in eq 1 result in the overall energy shift for a homogeneous ensemble of pinned molecules,[25] so we neglect them in the following.

The effective ED interaction in the form of eq (1) can be used in combination with eqs 2 and 3 to classify the different qubit encodings. To this end, we first note that if $J_z = 0$ and $J_\perp = 0$, the ED interaction between the qubits is identically zero. According to eq 1, the vanishing of the ED interaction requires the following two conditions to be simultaneously fulfilled: $d_\uparrow = d_\downarrow$ and $d_{\uparrow\downarrow} = 0$. Thus, all qubit encodings, for which the diagonal elements of the EDM are equal and the off-diagonal matrix elements vanish, will have zero ED interaction. Because of this, we expect such qubit encodings to have long coherence times, which can be advantageous for long-term quantum information storage (memory qubits).

We use a pair of categorical variables Z and X to characterize the encodings based on eq (1). The variable Z takes the value of 0 if the Ising interaction is zero ($J_z = 0$) and 1 otherwise. Similarly, the variable X takes the value of 0 if the spin-exchange interaction is zero ($J_\perp = 0$) and 1 otherwise. This gives rise to four possible encodings listed in Table 1. For example, the encoding, for which $J_z = J_\perp = 0$, is classified as 0/0. We can also refer to it as noninteracting because, as

https://doi.org/10.1021/acs.jpca.3c02835
J. Phys. Chem. A 2023, 127, 6593−6602

Table 1. Qubit Encoding Classification Based on the Effective ED Interqubit Coupling

qubit type	examples	advantages	limitations
0/0 (noninteracting)	nuclear spin sublevels ($N = 0$)	coherence time	two-qubit gates
$d_\uparrow = d_\downarrow$, $d_{\uparrow\downarrow} = 0$	nonadjacent rotational states, $E = 0$	QI storage	
0/1 (spin-exchange)	adjacent rotational states, $E = 0$[a]	two-qubit gates	coherence time
$d_\uparrow = d_\downarrow$, $d_{\uparrow\downarrow} \neq 0$		entanglement	
1/0 (Ising)	rotational-spin states ($N = 0, 1$)[b]	two-qubit gates	coherence time
$d_\uparrow \neq d_\downarrow$, $d_{\uparrow\downarrow} = 0$	nonadjacent rotational states[c]	entanglement	
1/1 (XXZ)	adjacent rotational states, $E > 0$[a]	two-qubit gates	coherence time
$d_\uparrow \neq d_\downarrow$, $d_{\uparrow\downarrow} \neq 0$	nonadjacent rotational states, $E > 0$[d]	entanglement	

[a]With the same spin projection ($M = M'$). [b]With different spin projections ($M \neq M'$). [c]With $|\Delta M_N| \geq 2$ regardless of M and M'. [d]With $|\Delta M_N| \leq 1$ and the same spin projection ($M = M'$).

shown above, the qubit states are not coupled by the long-range ED interaction.

As an example of the 0/0 encoding, consider the nuclear spin sublevels of the ground ($N = 0$) rotational state of alkali-dimer molecules. In the high magnetic field limit, the eigenstates of these molecules can be written as $|NM_N\rangle|I_1M_{I_1}\rangle|I_2M_{I_2}\rangle = |NM_N, M\rangle$, where $|NM_N\rangle$ are the eigenstates of rotational angular momentum $\hat{N}$ and its z-component $\hat{N}_z$, $|I_\alpha\ M_{I_\alpha}\rangle$ are the eigenstates of the nuclear spin operators $\hat{I}_\alpha^2$ and $\hat{I}_{\alpha_z}$ of the α-th nucleus ($\alpha = 1, 2$), and $M = \{M_{I_1}, M_{I_2}\}$ is a collective nuclear spin quantum number.[27] The nuclear spin qubit states are then encoded as $|\uparrow\rangle = |00, M\rangle$ and $|\downarrow\rangle = |00, M'\rangle$ with $M \neq M'$. With this encoding, $d_\uparrow = d_\downarrow$ because both the $|\uparrow\rangle$ and $|\downarrow\rangle$ states have $N = 0$ and $d_{\uparrow\downarrow} = 0$ because the EDM operators $\hat{d}$ and $\hat{d}_\pm$ are diagonal in the nuclear spin quantum number (for concreteness, we focus on the $q = 0$ spherical tensor component of the EDM operator $\hat{d} = \hat{d}_0$, noting that the $q = \pm 1$ components can be treated in a similar way)

$$\langle NM_N, M|\hat{d}|N'M'_N, M'\rangle = \langle NM_N|\hat{d}|N'M'_N\rangle\delta_{MM'} \tag{6}$$

and the nuclear spin qubit states have $M \neq M'$. In the presence of an external dc electric field E, the expectation values $d_\uparrow$ and $d_\downarrow$ are different from zero, but $d_\uparrow = d_\downarrow$, so both J_z and $J_\perp$ vanish even at $E > 0$. This effectively cancels the long-range ED interactions, leading to long coherence times of several seconds or longer, as observed experimentally for ultracold trapped KRb,[19,28] RbCs,[14] NaK,[13] and NaRb[29] molecules.

As noted above, in order for two qubits to interact via the long-range ED interaction (1), either J_z or $J_\perp$ (or both) must be nonzero. This leads to three other types of encodings listed in Table 1, which we now proceed to analyze.

First, if $J_z = 0$ and $J_\perp \neq 0$, the effective spin−spin interaction between the ith and jth qubits (1) takes the form of the long-range spin-exchange interaction[24−26]

$$H_{ij} = \frac{1 - 3\cos^2\theta_{ij}}{R_{ij}^3}\left[\frac{J_\perp}{2}(S_i^+S_j^- + \text{h. c.})\right] \tag{7}$$

Because $J_\perp \neq 0$ and $J_z = 0$, this encoding can be classified as 0/1 (see Table 1). This is by far the most common type of encoding considered in the literature to date. As an example, the encoding into adjacent rotational states $|\uparrow\rangle = |00, M\rangle$ and $|\downarrow\rangle = |1M_N, M'\rangle$ with $M = M'$ was originally proposed in a seminal paper by DeMille.[5] It follows from eq 6 that the off-diagonal EDM matrix element does not vanish

$$d_{\uparrow\downarrow} = \langle 00, M|\hat{d}|1M_N, M\rangle = \langle 00|\hat{d}|1M_N\rangle \neq 0 \tag{8}$$

and hence, $J_\perp \propto d_{\uparrow\downarrow}^2 \neq 0$. The diagonal EDM matrix elements in the adjacent rotational state encoding are zero in the absence of an external E-field because the two rotational states have a definite parity. As a result, $J_z = 0$ and the adjacent rotational state encoding can be classified as 0/1. In a nonzero electric field, $d_\uparrow \neq d_\downarrow$, and thus, $J_z \neq 0$ and the type of encoding changes to 1/1 (see below). This demonstrates that applying an external E-field can cause interconversion between the different types of encodings. We will see another example of this "encoding crossover" in Section 3.

Second, if $J_z \neq 0$ and $J_\perp = 0$, the effective spin−spin interaction between the ith and jth qubits 1 takes the form of the long-range Ising interaction[10]

$$H_{ij} = \frac{1 - 3\cos^2\theta_{ij}}{R_{ij}^3}J_zS_i^zS_j^z \tag{9}$$

Because $J_z \neq 0$ and $J_\perp = 0$, this is a 1/0 encoding (see Table 1). Until very recently, this type of encoding has been virtually unexplored, unlike the standard 0/0 and 0/1 encodings.[5,14] One example of such encoding, which we will refer to as rotational-spin, can be realized by the lowest two rotational states with *different* nuclear spin projections,[10] i.e., $|\uparrow\rangle = |00, M\rangle$ and $|\downarrow\rangle = |1M_N, M'\rangle$ with $M \neq M'$ (note that in the standard encoding into adjacent rotational states, $M = M'$).

Equation 9 shows that encodings of the 1/0 type, such as the rotational-spin encoding, naturally give rise to the long-range Ising interaction.[10] Dynamical evolution of quantum many-body systems interacting via the Ising Hamiltonian generates cluster-state entanglement.[30] Cluster states are universal entangled resource states for measurement-based quantum computation.[30,31] The Ising interaction (9) can also be used to implement universal two-qubit quantum logic gates (Ising gates), which have been explored in the context of nuclear magnetic resonance (NMR)-based quantum computation.[32] These interactions can also be used for more complex QI protocols, such as, for example, protocols based on qubits encoded into states of multiple molecules, which can be used for engineering transverse-field Ising models for applications such as quantum annealing.[21]

Finally, when both $J_\perp$ and J_z are nonzero, the effective spin−spin interaction contains both the Ising and spin-exchange terms, leading to the 1/1 type encoding, in which all of the terms in the XXZ Hamiltonian are nonzero. As stated above, one common example of such encoding is furnished by the adjacent rotational states with the same nuclear spin projection ($|\uparrow\rangle = |00, M\rangle$ and $|\downarrow\rangle = |1M_N, M'\rangle$ with $M = M'$) in a nonzero electric field (in Section 3, we will consider a less familiar example of encoding into nonadjacent rotational states). In this encoding, $d_{\uparrow\downarrow} \neq 0$ and the presence of the field ensures that $d_\uparrow$

https://doi.org/10.1021/acs.jpca.3c02835
J. Phys. Chem. A 2023, 127, 6593−6602

$\neq d_\uparrow$, and thus, $J_z \neq 0$. The property of both the Ising and spin-exchange interactions being different from zero is advantageous for a number of applications, such as dynamical generation of many-body spin-squeezed states,[9,10] which can be used to achieve metrological gain over the standard quantum limit.[33,34] At the same time, the coherence properties of 1/1 type qubits (as well as those of the 1/0 and 0/1 types) may be limited by the strong and long-range ED interaction, which is experimentally challenging to turn on and off.

3. QUBIT ENCODING INTO NONADJACENT ROTATIONAL LEVELS

To illustrate the application of the proposed classification scheme, we consider qubit encoding into nonadjacent rotational levels of a $^1\Sigma$ molecule. A similar type of encoding was briefly mentioned in ref 24. The Hamiltonian of a $^1\Sigma$ molecule in the vibrational ground state placed in a dc electric field $\boldsymbol{E}$ can be written as

$$\hat{H} = B_e\hat{N}^2 - \boldsymbol{E}\cdot\boldsymbol{d} \tag{10}$$

where B_e is the rotational constant and $\boldsymbol{d}$ is the dipole moment of the molecule. Figure 1 shows the lowest nine eigenvalues of

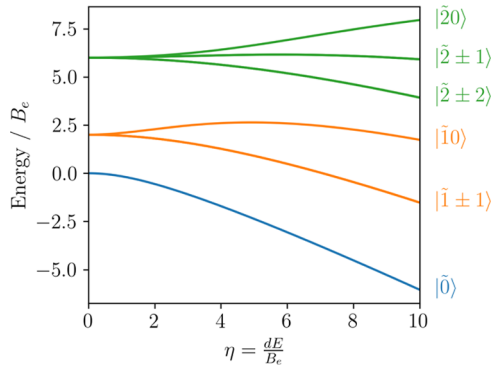

Figure 1. Energy levels of a $^1\Sigma$ molecule as functions of the effective electric field.

Hamiltonian 10 as functions of the effective electric field $\eta \equiv dE/B_e$. These states correspond to rotational states with $N = 0$, 1, and 2 at the zero field.

The interaction of molecules with the electric field couple rotational states $|NM_N\rangle$ with the same projection (M_N) to yield dc field-dressed (or pendular) states[25,35]

$$|\tilde{N}M_N\rangle = \sum_N c_N|NM_N\rangle \tag{11}$$

The choice of $|\uparrow\rangle = |\tilde{0}0\rangle$ leaves five choices for $|\downarrow\rangle$ from the manifold correlating at zero field with $N = 2$, including $|\tilde{2}0\rangle$, $|\tilde{2}\pm1\rangle$, and $|\tilde{2}\pm2\rangle$. The matrix elements of the dipole operators in the rotational basis states are calculated as

$$\langle N'M_{N'}|\hat{d}_p|NM_N\rangle = d(-1)^{M_{N'}}\sqrt{(2N'+1)(2N+1)}\begin{pmatrix} N' & 1 & N \\ -M_{N'} & p & M_N\end{pmatrix}\begin{pmatrix} N' & 1 & N \\ 0 & 0 & 0\end{pmatrix} \tag{12}$$

where d is the permanent dipole moment of the molecule. The 3j-symbols in eq 12 vanish if $|N' - N| > 1$ and $M_N + p \neq M_{N'}$.

The nonzero EDM matrix elements of $\hat{d}_0$ as a function of the effective electric field $\eta \equiv dE/B_e$ are displayed for the three possible encodings in Figure 2, where

$$d_\uparrow = \langle\tilde{0}0|\hat{d}_0|\tilde{0}0\rangle \tag{13}$$

$$d_\downarrow^{(NM_N)} = \langle\tilde{N}M_N|\hat{d}_0|\tilde{N}M_N\rangle \tag{14}$$

$$d_{\uparrow\downarrow}^{(NM_N)} = \langle\tilde{0}0|\hat{d}_0|\tilde{N}M_N\rangle \tag{15}$$

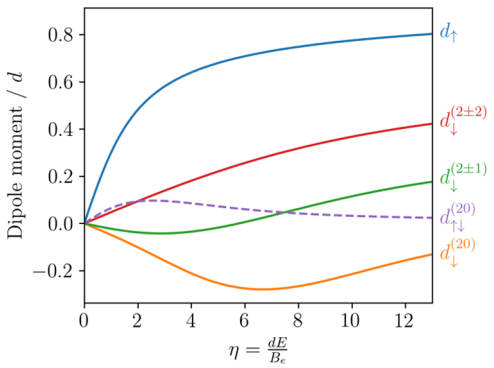

Figure 2. Nonzero EDM matrix elements of $\hat{d}_0$ for a $^1\Sigma$ molecule as a function of the effective electric field $\eta = \frac{dE}{B_e}$.

The transition matrix elements of $\hat{d}_p$ ($d_{\uparrow\downarrow}$ and $d_{\uparrow\downarrow}^{\pm}$) vanish for states with $M_N \neq p$. Therefore, $d_{\uparrow\downarrow}$ is only nonzero when $|\downarrow\rangle = |\tilde{2}0\rangle$ and $d_{\uparrow\downarrow}^{\pm}$ is only nonzero when $|\downarrow\rangle = |\tilde{2}\pm1\rangle$. Note that $d_{\uparrow\downarrow} \neq 0$ at $E > 0$ because the states $|\tilde{0}0\rangle$ and $|\tilde{2}0\rangle$ couple through the intermediate state $|\tilde{1}0\rangle$. All transition dipole matrix elements vanish for $|\downarrow\rangle = |\tilde{2}\pm2\rangle$. All diagonal matrix elements are zero for bare rotational states at zero field.

As follows from Figure 2, qubits spanning the $\tilde{N} = 0$ and $\tilde{N} = 2$ pairs permit three classes of encoding: the 0/0 encoding at a vanishing electric field, 1/0 encoding, and 1/1 encoding, depending on the $|\uparrow\rangle$ state. To illustrate this more clearly, we calculate the parameters of the XXZ interaction of eq 1 using eqs (2) and (3) and the EDM matrix elements. Figure 3 shows the couplings J_z and $J_\perp$ as functions of the effective electric field. As described in eq 2, the Ising coupling between qubits grows as a function of the difference between the diagonal matrix elements of the EDM in the qubit basis. This is observed in the left panel of Figure 3, as J_z is consistently maximized for $|\downarrow\rangle = |\tilde{2}0\rangle$. On the other hand, $J_\perp$ corresponds to the square of the off-diagonal EDM matrix elements. As expected, $J_\perp$ is equal to zero when $|\downarrow\rangle = |\tilde{2}2\rangle$ regardless of the E-field, while $J_\perp$ is positive for $|\downarrow\rangle = |\tilde{2}0\rangle$ and negative for $|\downarrow\rangle = |\tilde{2}0\rangle$ at a nonzero E-field. An avoided crossing between states $|20\rangle$ and $|30\rangle$ at $\eta \approx 18$ complicates the couplings at stronger fields, with abrupt changes in the couplings to the $|20\rangle$ state. However, both perpendicular couplings are maximized at intermediate field strengths and diminish to zero in strong fields.

Comparing the relative magnitudes of $J_\perp$ and J_z in the nonadjacent vs. adjacent rotational state encodings, we note that $J_\perp$ is significantly weaker in the former encoding scheme due to the smaller magnitude of $d_{\uparrow\downarrow}$ [see eq 3]. However, the J_z couplings are of a similar magnitude because they depend on the difference between the expectation values $d_\uparrow$ and $d_\downarrow$ [see eq 2], which are similar in both types of encoding.

https://doi.org/10.1021/acs.jpca.3c02835
J. Phys. Chem. A 2023, 127, 6593−6602

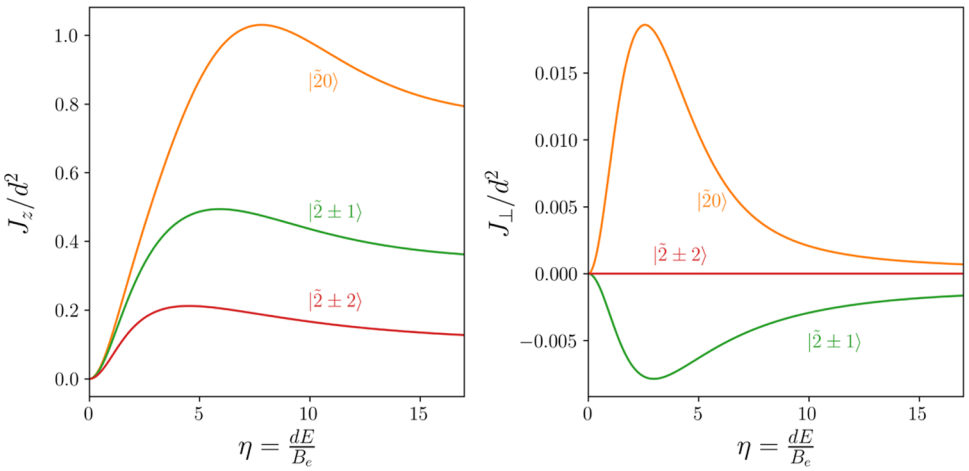

Figure 3. Couplings J_z (left) and $J_\perp$ (right) as a function of the effective electric field $\eta = \frac{dE}{B_e}$, using the ground rotational state and the indicated rotational states of a polar $^1\Sigma$ molecule to encode the qubits.

4. QUADRUPOLE−QUADRUPOLE INTERACTION

The classification scheme proposed here can be extended to other long-range interactions compared to the ED interaction. As an example, we consider in the present section the quadrupole−quadrupole (QQ) interaction. This interaction is the leading long-range interaction between homonuclear molecules, which simultaneously possess even/odd N state manifolds and which therefore can particularly benefit from the qubit encoding introduced in the preceding section. Previous theoretical work has shown that QQ interactions of nonpolar atoms and molecules in two-dimensional optical lattices can give rise to exotic topological phases.[36]

As shown in Appendix B, the QQ interaction leads to the same XXZ model as given by eq (1). However, the model parameters must now be expressed in terms of the matrix elements of the quadrupole moment, yielding the following relations:

$$J_z = (q_\uparrow - q_\downarrow)^2 \tag{16}$$

$$J_\perp = 2[6q_{\uparrow\downarrow}^2 - 4[|q_{\uparrow\downarrow}^{+1}|^2 + |q_{\uparrow\downarrow}^{-1}|^2] + [|q_{\uparrow\downarrow}^{+2}|^2 + |q_{\uparrow\downarrow}^{-2}|^2]] \tag{17}$$

Thus, the same classification scheme can be applied to qubits encoded in nonpolar molecules interacting through QQ couplings with analogous conditions on the vanishing of J_z and $J_\perp$, which can be analyzed by considering the matrix elements of the quadrupole moment in the single-molecule basis.

These matrix elements are

$$\langle N'M_{N'}|\hat{q}_p|NM_N\rangle = q(-1)^{M_{N'}}\sqrt{(2N'+1)(2N+1)} \times \begin{pmatrix} N' & 2 & N \\ -M_{N'} & p & M_N \end{pmatrix} \begin{pmatrix} N' & 2 & N \\ 0 & 0 & 0 \end{pmatrix} \tag{18}$$

where q is the permanent quadrupole moment of the molecule. The 3j-symbols in eq 18 vanish if $|N' - N| > 2$ and $M_N + p \neq M_{N'}$. The nonzero EDM matrix elements of $\hat{q}_0$ as a function of the effective electric field $\eta \equiv \frac{dE}{B_e}$ are displayed for the three possible encodings in Figure 4, where

$$q_\uparrow = \langle\tilde{0}0|\hat{q}_0|\tilde{0}0\rangle \tag{19}$$

$$q_\downarrow^{(NM_N)} = \langle\tilde{N}M_N|\hat{q}_0|\tilde{N}M_N\rangle \tag{20}$$

$$q_{\uparrow\downarrow}^{(NM_N)} = \langle\tilde{0}0|\hat{q}_0|\tilde{N}M_N\rangle \tag{21}$$

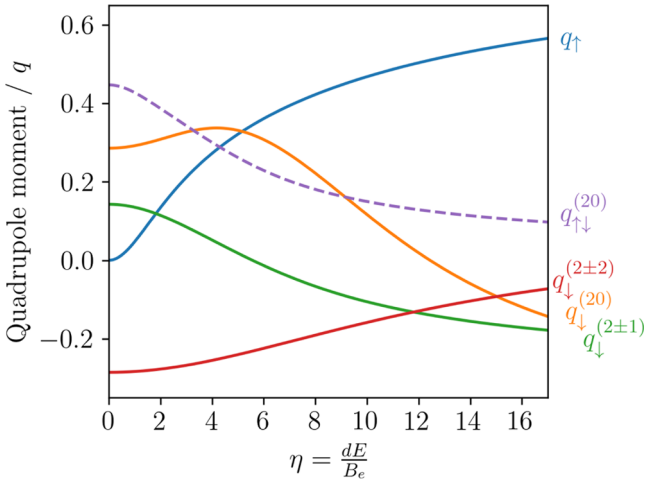

Figure 4. Nonzero matrix elements of $\hat{q}_0$ as functions of the effective electric field $\eta = \frac{dE}{B_e}$.

The transition matrix elements of $\hat{q}_p$ ($q_{\uparrow\downarrow}$, $q_{\uparrow\downarrow}^{\pm1}$, and $q_{\uparrow\downarrow}^{\pm2}$) vanish for states with $M_N \neq p$. Therefore, $q_{\uparrow\downarrow}$ is only nonzero when $|\downarrow\rangle = |\tilde{2}0\rangle$. $q_{\uparrow\downarrow}^{\pm1}$ is only nonzero when $|\downarrow\rangle = |\tilde{2}\pm1\rangle$, and $q_{\uparrow\downarrow}^{\pm2}$ is only nonzero when $|\downarrow\rangle = |\tilde{2}\pm2\rangle$.

To illustrate the possible types of encoding achievable with homonuclear molecules, we calculate the parameters of the XXZ interaction of eq 1 using eqs 16 and 17 and the quadrupole matrix elements. Figure 5 shows the QQ couplings J_z and $J_\perp$ as functions of the effective electric field for a polar molecule. As described in eq 16, the Ising coupling between qubits grows as a function of the difference in the diagonal matrix elements of the EDM. On the other hand, $J_\perp$ corresponds to the square of the off-diagonal quadrupole matrix elements. As expected, $J_\perp$ is positive for $|\downarrow\rangle = |\tilde{2}0\rangle$ and $|\downarrow\rangle = |\tilde{2}\pm2\rangle$ and negative for $|\downarrow\rangle = |\tilde{2}\pm1\rangle$ at the nonzero E-

https://doi.org/10.1021/acs.jpca.3c02835
J. Phys. Chem. A 2023, 127, 6593−6602

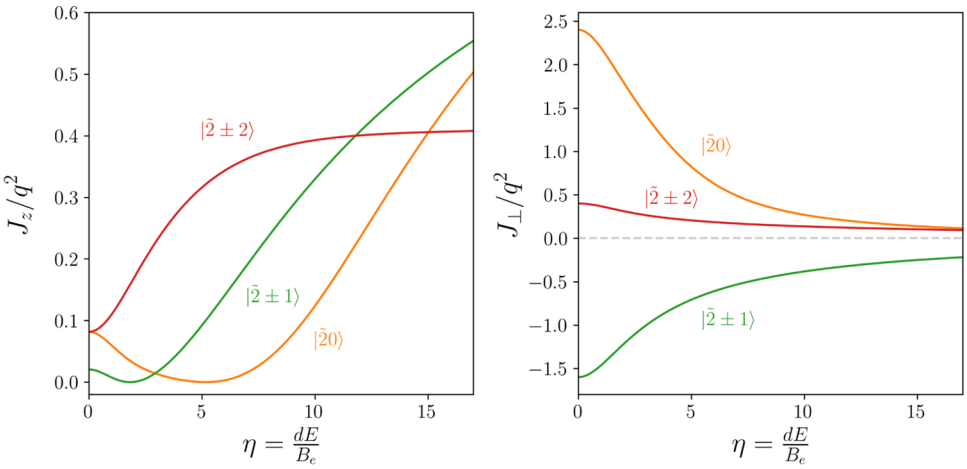

Figure 5. Quadrupole contribution to couplings J_z (left) and $J_\perp$ (right) as a function of the effective electric field $\eta = \frac{dE}{B_e}$, using the ground rotational state and the indicated rotational states to encode the qubits.

field. However, all three perpendicular couplings are maximized at zero field strengths and diminish to zero in strong fields. It can be observed that the QQ interaction permits the following types of encoding based on the $\tilde{N} = 0$ and $\tilde{N} = 2$ states: 0/1, 1/1, and 1/0.

Finally, we note that for typical lattice spacings used in current experiments ($\simeq$ 500−1000 nm), the QQ interaction is on the order of $\lesssim$1 Hz, which is two-three orders of magnitude weaker than the ED interaction between polar molecules. Despite its weakness, the effective QQ interaction Hamiltonian has the same form as the ED Hamiltonian, and can therefore be used (at least in principle) to generate useful many-body entangled states of nonpolar molecules in the same way as the ED interaction of polar molecules.[9,10] In order to ensure robust dynamical evolution toward such entangled states, the evolution timescale should be much shorter than the coherence time of nonadjacent rotational state superpositions.[8,10]

5. CONCLUSIONS

Molecules are complex quantum systems that feature multiple energy scales ranging from tens of Hz (hyperfine, Zeeman, and tunneling doublet structure) to thousands of THz (electronic structure). In addition, intermolecular interactions at short range are described by multidimensional potential energy surfaces (PESs), whose accurate description requires sophisticated quantum chemistry techniques and fitting methods. However, the long-range physics of intermolecular interactions of relevance to current QIS experiments in optical lattices and tweezers[1,2] is completely described by the well-established multipole expansion. The lowest leading order in the multipole expansion for neutral (uncharged) polar molecules is represented by the ED interaction and the next leading orders by the EQ and QQ interactions.

For qubit-based QIS applications, the molecule is reduced to a two-level system (the qubit), whose effective spin-1/2 levels can be encoded into the electronic, vibrational, rotational, fine, hyperfine, Stark, or Zeeman states. Different choices of encoding give rise to different flavors of the ED interaction between the qubits. Here, we have shown that all possible encodings can be classified into 4 types based on the flavor of the effective ED interaction they give rise to.

Our classification is based on two realizations. First, the general interaction between molecular qubits is completely determined by the ED Hamiltonian in the effective two-qubit basis. Second, the form of this Hamiltonian depends only on the matrix elements of the EDM of the individual molecules in a given encoding. The general ED Hamiltonian takes the form of the iconic XXZ Heisenberg model of quantum magnetism[25] with the Ising and spin-exchange coupling parameters J_z and $J_\perp$ expressed in terms of the diagonal ($d_\uparrow$, $d_\downarrow$) and off-diagonal ($d_{\uparrow\downarrow}$) EDM matrix elements of each of the individual molecules. As a result, the flavor of the ED interaction is completely determined by single-molecule EDM matrix elements in the qubit basis, regardless of the precise nature of qubit states.

The versatility of our proposed classification scheme is based on mapping the ED and QQ interactions to the XXZ Hamiltonian. In principle, higher-n multipole interactions between molecules would allow for a similar mapping because each radial term in the multipole expansion is multiplied by a product of the individual molecules' multipole moments.[37] However, these higher-n multipole interactions scale with higher powers of $1/R$ and hence are hundreds of times smaller than the already small QQ interaction for typical lattice spacings considered here.

It follows from eq 1 that there can be 4 flavors of the ED interaction depending on whether or not the coupling constants J_z and $J_\perp$ are equal to zero. If $J_z = J_\perp = 0$, no ED interaction is present between the qubits, and we classify them as noninteracting (0/0). In the latter case, three types of the ED interaction can be distinguished based on whether the values of $|d_\uparrow - d_\downarrow|$ and $d_{\uparrow\downarrow}$ are zero (see Table 1). We classify these three types as Ising (1/0), spin-exchange (0/1), and XXZ (1/1).

To identify the type of molecular qubit encoding, the reader can use the diagram shown in Figure 6. One begins by calculating the matrix elements of the EDM in the qubit basis $d_\uparrow$, $d_\downarrow$, and $d_{\uparrow\downarrow}$ and locating the corresponding box on the left-hand side of the diagram. The right-hand side of the diagram identifies the type of qubit encoding and outlines its possible applications, with a more detailed discussion provided in Section 2.

To illustrate our classification scheme, we have considered a new type or molecular qubit encoding into nonadjacent

https://doi.org/10.1021/acs.jpca.3c02835
J. Phys. Chem. A 2023, 127, 6593−6602

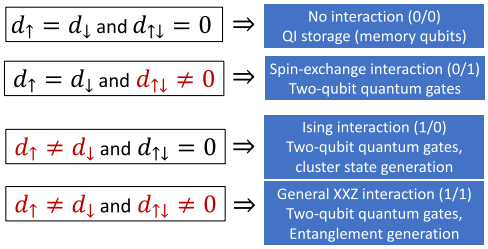

Figure 6. Molecular qubit encoding classification diagram. To classify a qubit, determine the values of $d_\uparrow$, $d_\downarrow$, and $d_{\uparrow\downarrow}$ and locate the relevant box in the left column. The qubit encoding type is indicated to the right of each box.

rotational states of a polar diatomic molecule (such as $N = 0$ and $N = 2$). At zero external electric field, all EDM matrix elements vanish due to the parity selection rules, and this encoding can be classified as noninteracting (or 0/0 type). In the presence of a dc electric field, the qubit is converted into type 1/1 due to both diagonal and off-diagonal EDM matrix elements being nonzero. However, when the projection M_N of the rotational angular momentum of the qubit states differs by two or more, the off-diagonal matrix elements of the EDM vanish identically, and the encoding type changes to 1/0.

It should be noted that our classification is based on the electric multipole interactions and thus excludes magnetic interactions, which can be substantial for open-shell molecular radicals bearing magnetic moments, such as CaF($^2\Sigma^+$), SrF($^2\Sigma^+$), YO($^2\Sigma^+$), and NaLi($a^3\Sigma^+$), which have recently been cooled and confined in magnetic and optical dipole traps.[38−45] The leading-order magnetic dipole−dipole (MD) interaction scales as α^2/R_{ij}^3, where α is the fine-structure constant. At a typical optical lattice spacing $R_{ij} = 500$ nm, the strength of the MD interaction is 0.42 Hz, which is comparable to the electric QQ interaction. The utility of the MD interaction has been pointed out in the context of quantum information processing[46] and quantum simulation[47,48] with magnetic atoms trapped in optical lattices. We envision that the intermolecular MD interaction could be used in the same way to, e.g., engineer quantum logic gates between trapped magnetic molecules. It would be particularly interesting to explore this possibility with highly magnetic molecules such as CrH($^6\Sigma^+$) and MnH($^7\Sigma^+$),[49] whose MD interactions are enhanced by several orders of magnitude compared to the above estimate, making them comparable to the ED interactions.

In future work, it would be interesting to apply our classification to identify novel encodings of molecular qubits, which could prove useful for QIS applications. There remain pairs of molecular states, which have not been explored for qubit encoding, such as the hyperfine components of different electronic and rovibrational states. It would also be interesting to extend our scheme to classify qubit encodings in polyatomic molecules,[4,50] which have recently been cooled and trapped in several laboratories.[51−54] It may also be fruitful to explore the electric dipole−quadrupole interaction, which is activated only when the molecules are prepared in different types of rotational encodings (e.g., one half in a coherent superposition of the $N = 0$ and 1 rotational states and the other half in that of the $N = 0$ and 2 states). These cross-encoding interactions could prove useful for engineering interactions in ultracold two-component mixtures of polar and nonpolar molecular gases.

APPENDIX A: EFFECTIVE ELECTRIC DIPOLE−DIPOLE INTERACTION

The ED interaction between molecules i and j takes the form[55]

$$H_{ij} = R_{ij}^{-3}\left[-\frac{3}{2}\sin^2\theta(\hat{d}_1\hat{d}_1 e^{-2i\phi} + \text{h.c.}) - \frac{3}{\sqrt{2}}\sin\theta\cos\theta[(\hat{d}_1\hat{d}_0 + \hat{d}_0\hat{d}_1)e^{-i\phi} + \text{h.c.}] - \frac{1}{2}(3\cos^2\theta - 1)(2\hat{d}_0\hat{d}_0 + \hat{d}_1\hat{d}_{-1} + \hat{d}_{-1}\hat{d}_1)\right] \tag{22}$$

where $\hat{d}_p$ are the spherical components of the dipole operator ($\hat{d}_0 = \hat{d}_z$, $\hat{d}_{\pm1} = \mp(\hat{d}_x \pm i\hat{d}_y)/\sqrt{2}$), R_{ij} is the distance between the molecules, and θ_{ij} is the angle between the quantization vector and the vector connecting the two molecules. As the ED interaction is typically much weaker than the energy difference between the two qubit states $|\uparrow\rangle$, $|\downarrow\rangle$, processes that change the total magnetization are energetically off-resonant and can be neglected. With this assumption, the ED interaction can be described as the following spin Hamiltonian in the space spanned by $\{|\uparrow\uparrow\rangle, |\uparrow\downarrow\rangle, |\downarrow\uparrow\rangle, |\downarrow\downarrow\rangle\}$

$$H_{ij} = \frac{1 - 3\cos^2\theta_{ij}}{R_{ij}^3}\left[\frac{J_\perp}{2}(S_i^+S_j^- + \text{h.c.}) + J_z S_i^z S_j^z + W(\mathbb{I}_i S_j^z + S_i^z \mathbb{I}_j) + V\mathbb{I}_i\mathbb{I}_j\right] \tag{23}$$

The dipole−dipole interaction of eq 22 can be seen as a sum of terms that transfer $-2 < q < 2$ units of rotational angular momentum projection to the molecules' angular momentum projection. Assuming that states of different M_N are not mixed together, terms with $q \neq 0$ are energetically off-resonant and eq 22 can be simplified to only include terms with $q = 0$:

$$H_{ij} = \frac{1 - 3\cos^2\theta_{ij}}{2R_{ij}^3}(2\hat{d}_0\hat{d}_0 + \hat{d}_1\hat{d}_{-1} + \hat{d}_{-1}\hat{d}_1) \tag{24}$$

Ignoring energetically off-resonant terms of H_{ij}, the interaction matrix can be written as

$$\mathbf{H}_{ij} = \frac{1 - 3\cos^2\theta}{R_{ij}^3}\begin{pmatrix} H_{11} & 0 & 0 & 0 \\ 0 & H_{22} & H_{23} & 0 \\ 0 & H_{23}^* & H_{33} & 0 \\ 0 & 0 & 0 & H_{44} \end{pmatrix} \tag{25}$$

To evaluate the couplings in eq 23, we need to first define the matrix elements of the interaction Hamiltonian. We define $d_\uparrow$, $d_\downarrow$, $d_{\uparrow\downarrow}$, and $d_{\uparrow\downarrow}^\pm$ as the matrix elements of the dipole operators

$$\langle\uparrow|\hat{d}_0|\uparrow\rangle \equiv d_\uparrow, \langle\downarrow|\hat{d}_0|\downarrow\rangle \equiv d_\downarrow \tag{26}$$

$$\langle\uparrow|\hat{d}_0|\downarrow\rangle \equiv d_{\uparrow\downarrow}, \langle\uparrow|\hat{d}_{\pm1}|\downarrow\rangle \equiv d_{\uparrow\downarrow}^\pm \tag{27}$$

The matrix elements of H_{ij}, under the assumptions of eq 24 become

$$H_{11} = \langle\uparrow\uparrow|d_0 d_0|\uparrow\uparrow\rangle = d_\uparrow^2 \tag{28}$$

$$H_{44} = \langle\downarrow\downarrow|d_0 d_0|\downarrow\downarrow\rangle = d_\downarrow^2 \tag{29}$$

$$H_{22} = H_{33} = \langle\uparrow\downarrow|d_0 d_0|\uparrow\downarrow\rangle = d_\uparrow d_\downarrow \tag{30}$$

https://doi.org/10.1021/acs.jpca.3c02835
J. Phys. Chem. A 2023, 127, 6593−6602

$$H_{23} = \langle \uparrow \downarrow | d_0 d_0 | \downarrow \uparrow \rangle + \frac{1}{2}[\langle \uparrow \downarrow | d_1 d_{-1} | \downarrow \uparrow \rangle + \langle \uparrow \downarrow | d_{-1} d_1 | \downarrow \uparrow \rangle]$$
$$= d_{\uparrow\downarrow}^2 + \frac{1}{2}[d_{\uparrow\downarrow}^+ d_{\downarrow\uparrow}^- + d_{\uparrow\downarrow}^- d_{\downarrow\uparrow}^+]$$
$$= d_{\uparrow\downarrow}^2 - \frac{1}{2}[|d_{\uparrow\downarrow}^+|^2 + |d_{\uparrow\downarrow}^-|^2] \quad (31)$$

Since $\hat{d}_{\pm 1} = -\hat{d}_{\mp 1}^\dagger$, we get $d_{\uparrow\downarrow}^+ = -(d_{\downarrow\uparrow}^-)^*$ and $d_{\downarrow\uparrow}^+ = -(d_{\uparrow\downarrow}^-)^*$. The couplings of eq 23 are then derived as

$$J_z = H_{11} - H_{22} - H_{33} + H_{44}$$
$$= (d_\uparrow - d_\downarrow)^2 \quad (32)$$

$$J_\perp = 2H_{23}$$
$$= 2d_{\uparrow\downarrow}^2 - |d_{\uparrow\downarrow}^+|^2 - |d_{\uparrow\downarrow}^-|^2 \quad (33)$$

$$W = \frac{1}{2}(H_{11} - H_{44})$$
$$= (d_\uparrow^2 - d_\downarrow^2)/2 \quad (34)$$

$$V = \frac{1}{4}(H_{11} + H_{22} + H_{33} + H_{44})$$
$$= (d_\uparrow + d_\downarrow)^2/4 \quad (35)$$

in terms of the dipole matrix elements of eqs 4 and 5. Therefore, we observe that while all four terms depend on the matrix elements of the $\hat{d}_0$ operator, $J_\perp$ is also affected by the transition dipole matrix elements of $\hat{d}_{\pm 1}$.

APPENDIX B: EFFECTIVE ELECTRIC QUADRUPOLE−QUADRUPOLE INTERACTION

The quadrupole−quadrupole interaction between molecules i and j takes the form

$$H_{ij} = R_{ij}^{-5}\left[\frac{35}{8}\sin^4\theta\,(q_2 q_2 e^{4i\phi} + \text{h.c.}) + \frac{15}{4}\sqrt{7}\,\sin^3\theta\cos\theta[(q_2 q_1 + q_1 q_2)e^{-3i\phi} + \text{h.c.}] + \frac{5}{4}\sin^2\theta(7\cos^2\theta - 1)\left[\left(\sqrt{\frac{3}{2}}\,q_2 q_0 + \sqrt{\frac{3}{2}}\,q_0 q_2 + 2q_1 q_1\right)e^{2i\phi} + \text{h.c.}\right] + \frac{15}{4}\sin\theta\cos\theta\left(\frac{7}{3}\cos^2\theta - 1\right)[(q_2 q_{-1} + q_{-1} q_2 + \sqrt{6}\,q_1 q_0 + q_0 q_1)e^{i\phi} + \text{h.c.}] + \frac{3}{8}\left(\frac{35}{3}\cos^4\theta - 10\cos^2\theta + 1\right)[(q_2 q_{-2} + q_{-2} q_2 + 4(q_1 q_{-1} + q_{-1} q_1) + 6q_0 q_0)]\right] \quad (36)$$

where $\hat{q}_p$ are the spherical components of the quadrupole operator, R_{ij} is the distance between the molecules, and θ_{ij} is the angle between the quantization vector and the vector connecting the two molecules.

Using similar assumptions to 24, we can simplify 36 to only include terms with $q = 0$:

$$H_{ij} = R_{ij}^{-5}\left[\frac{3}{8}\left(\frac{35}{3}\cos^4\theta - 10\cos^2\theta + 1\right)[(q_2 q_{-2} + q_{-2} q_2 + 4(q_1 q_{-1} + q_{-1} q_1) + 6q_0 q_0)]\right] \quad (37)$$

Ignoring energetically off-resonant terms of H_{ij}, the interaction matrix can be written as

$$\mathbf{H}_{ij} = \frac{3}{8R_{ij}^5}\left(\frac{35}{3}\cos^4\theta - 10\cos^2\theta + 1\right)\begin{pmatrix} H_{11} & 0 & 0 & 0 \\ 0 & H_{22} & H_{23} & 0 \\ 0 & H_{23}^* & H_{33} & 0 \\ 0 & 0 & 0 & H_{44} \end{pmatrix} \quad (38)$$

We define $q_\uparrow$, $q_\downarrow$, $q_{\uparrow\downarrow}$, $q_{\uparrow\downarrow}^{\pm 1}$, and $q_{\uparrow\downarrow}^{\pm 2}$ as the matrix elements of the quadrupole operators

$$\langle \uparrow | \hat{q}_0 | \uparrow \rangle \equiv q_\uparrow, \quad \langle \downarrow | \hat{q}_0 | \downarrow \rangle \equiv q_\downarrow \quad (39)$$

$$\langle \uparrow | \hat{q}_0 | \downarrow \rangle \equiv q_{\uparrow\downarrow}, \quad \langle \uparrow | \hat{q}_{\pm 1} | \downarrow \rangle \equiv q_{\uparrow\downarrow}^{\pm 1} \quad (40)$$

$$\langle \uparrow | \hat{q}_{\pm 2} | \downarrow \rangle \equiv q_{\uparrow\downarrow}^{\pm 2} \quad (41)$$

The matrix elements of H_{ij}, under the assumptions of eq 37, become

$$H_{11} = 6\langle \uparrow \uparrow | q_0 q_0 | \uparrow \uparrow \rangle = 6q_\uparrow^2 \quad (42)$$

$$H_{44} = 6\langle \downarrow \downarrow | q_0 q_0 | \downarrow \downarrow \rangle = 6q_\downarrow^2 \quad (43)$$

$$H_{22} = H_{33} = 6\langle \uparrow \downarrow | q_0 q_0 | \uparrow \downarrow \rangle = 6q_\uparrow q_\downarrow \quad (44)$$

$$H_{23} = 6\langle \uparrow \downarrow | q_0 q_0 | \downarrow \uparrow \rangle + 4[\langle \uparrow \downarrow | q_1 q_{-1} | \downarrow \uparrow \rangle + \langle \uparrow \downarrow | q_{-1} q_1 | \downarrow \uparrow \rangle] + [\langle \uparrow \downarrow | q_2 q_{-2} | \downarrow \uparrow \rangle + \langle \uparrow \downarrow | q_{-2} q_2 | \downarrow \uparrow \rangle]$$
$$= 6q_{\uparrow\downarrow}^2 + 4[q_{\uparrow\downarrow}^{+1} q_{\downarrow\uparrow}^{-1} + q_{\uparrow\downarrow}^{-1} d_{\downarrow\uparrow}^{+1}] + [q_{\uparrow\downarrow}^{+2} q_{\downarrow\uparrow}^{-2} + q_{\uparrow\downarrow}^{-2} d_{\downarrow\uparrow}^{+2}]$$
$$= 6q_{\uparrow\downarrow}^2 - 4[|q_{\uparrow\downarrow}^{+1}|^2 + |q_{\uparrow\downarrow}^{-1}|^2] + [|q_{\uparrow\downarrow}^{+2}|^2 + |q_{\uparrow\downarrow}^{-2}|^2] \quad (45)$$

Since $\hat{q}_{\pm 1} = -\hat{q}_{\mp 1}^\dagger$ and $\hat{q}_{\pm 2} = \hat{q}_{\mp 2}^\dagger$, we get $q_{\uparrow\downarrow}^{+1} = -(q_{\downarrow\uparrow}^{-1})^*$, $q_{\uparrow\downarrow}^{+1} = -(q_{\downarrow\uparrow}^{-1})^*$, $q_{\uparrow\downarrow}^{+2} = (q_{\downarrow\uparrow}^{-2})^*$, and $q_{\uparrow\downarrow}^{+2} = (q_{\downarrow\uparrow}^{-2})^*$.

The effective QQ interaction Hamiltonian then takes the form of eq 23 (with the prefactor switched to that of eq 38) and the coupling constants

$$J_z = (q_\uparrow - q_\downarrow)^2 \quad (46)$$

$$J_\perp = 2[6q_{\uparrow\downarrow}^2 - 4[|q_{\uparrow\downarrow}^{+1}|^2 + |q_{\uparrow\downarrow}^{-1}|^2] + [|q_{\uparrow\downarrow}^{+2}|^2 + |q_{\uparrow\downarrow}^{-2}|^2]] \quad (47)$$

$$W = (q_\uparrow^2 - q_\downarrow^2)/2 \quad (48)$$

$$V = (q_\uparrow + q_\downarrow)^2/4 \quad (49)$$

https://doi.org/10.1021/acs.jpca.3c02835
J. Phys. Chem. A 2023, 127, 6593−6602

expressed in terms of the quadrupole matrix elements of eqs 39, 40, and 41. Therefore, we observe that while all four terms depend on the matrix elements of the $\hat{q}_0$ operator, $J_\perp$ is also affected by the transition dipole matrix elements of $\hat{q}_{\pm 1}$ and $\hat{q}_{\pm 2}$.

AUTHOR INFORMATION

Corresponding Author

Timur V. Tscherbul − *Department of Physics, University of Nevada, Reno, Nevada 89557, United States;* orcid.org/0000-0001-5689-040X; Email: ttscherbul@unr.edu

Authors

Kasra Asnaashari − *Department of Chemistry, University of British Columbia, Vancouver V6T 1Z1, Canada;* orcid.org/0000-0001-5176-3153

Roman V. Krems − *Department of Chemistry, University of British Columbia, Vancouver V6T 1Z1, Canada*

Complete contact information is available at: https://pubs.acs.org/10.1021/acs.jpca.3c02835

Notes

The authors declare no competing financial interest.

ACKNOWLEDGMENTS

The authors thank Ana Maria Rey for insightful discussions and for bringing to our attention the nonadjacent rotational state encoding. This work was supported by the NSF through the CAREER program (PHY-2045681). The work of KA and RVK is supported by NSERC of Canada.

REFERENCES

(1) Bohn, J. L.; Rey, A. M.; Ye, J. Cold molecules: Progress in quantum engineering of chemistry and quantum matter. *Science* **2017**, *357*, 1002−1010.

(2) Kaufman, A. M.; Ni, K.-K. Quantum science with optical tweezer arrays of ultracold atoms and molecules. *Nat. Phys.* **2021**, *17*, 1324−1333.

(3) Sawant, R.; Blackmore, J. A.; Gregory, P. D.; Mur-Petit, J.; Jaksch, D.; Aldegunde, J.; Hutson, J. M.; Tarbutt, M. R.; Cornish, S. L. Ultracold polar molecules as qudits. *New J. Phys.* **2020**, *22*, No. 013027.

(4) Albert, V. V.; Covey, J. P.; Preskill, J. Robust Encoding of a Qubit in a Molecule. *Phys. Rev. X* **2020**, *10*, No. 031050.

(5) DeMille, D. Quantum Computation with Trapped Polar Molecules. *Phys. Rev. Lett.* **2002**, *88*, No. 067901.

(6) Yelin, S. F.; Kirby, K.; Côté, R. Schemes for robust quantum computation with polar molecules. *Phys. Rev. A* **2006**, *74*, No. 050301.

(7) Ni, K.-K.; Rosenband, T.; Grimes, D. D. Dipolar exchange quantum logic gate with polar molecules. *Chem. Sci.* **2018**, *9*, 6830−6838.

(8) Micheli, A.; Brennen, G. K.; Zoller, P. A toolbox for lattice-spin models with polar molecules. *Nat. Phys.* **2006**, *2*, 341−347.

(9) Bilitewski, T.; De Marco, L.; Li, J.-R.; Matsuda, K.; Tobias, W. G.; Valtolina, G.; Ye, J.; Rey, A. M. Dynamical Generation of Spin Squeezing in Ultracold Dipolar Molecules. *Phys. Rev. Lett.* **2021**, *126*, No. 113401.

(10) Tscherbul, T. V.; Ye, J.; Rey, A. M. Robust Nuclear Spin Entanglement via Dipolar Interactions in Polar Molecules. *Phys. Rev. Lett.* **2023**, *130*, No. 143002.

(11) Holland, C. M.; Lu, Y.; Cheuk, L. W. On-Demand Entanglement of Molecules in a Reconfigurable Optical Tweezer Array. 2023, arXiv:2210.06309. arXiv.org e-Print archive. https://arxiv.org/abs/2210.06309 (accessed June 22).

(12) Bao, Y.; Yu, S. S.; Anderegg, L.; Chae, E.; Ketterle, W.; Ni, K.-K.; Doyle, J. M. Dipolar spin-exchange and entanglement between molecules in an optical tweezer array. 2023, arXiv:2211.09780. arXiv.org e-Print archive. https://arxiv.org/abs/2211.09780 (accessed June 22).

(13) Park, J. W.; Yan, Z. Z.; Loh, H.; Will, S. A.; Zwierlein, M. W. Second-scale nuclear spin coherence time of ultracold $^{23}Na^{40}K$ molecules. *Science* **2017**, *357*, 372−375.

(14) Gregory, P. D.; Blackmore, J. A.; Bromley, S. L.; Hutson, J. M.; Cornish, S. L. Robust storage qubits in ultracold polar molecules. *Nat. Phys.* **2021**, *17*, 1149−1153.

(15) Herrera, F.; Cao, Y.; Kais, S.; Whaley, K. B. Infrared-dressed entanglement of cold open-shell polar molecules for universal matchgate quantum computing. *New J. Phys.* **2014**, *16*, No. 075001.

(16) Karra, M.; Sharma, K.; Friedrich, B.; Kais, S.; Herschbach, D. Prospects for quantum computing with an array of ultracold polar paramagnetic molecules. *J. Chem. Phys.* **2016**, *144*, No. 094301.

(17) Tesch, C. M.; de Vivie-Riedle, R. Quantum Computation with Vibrationally Excited Molecules. *Phys. Rev. Lett.* **2002**, *89*, No. 157901.

(18) Zhao, M.; Babikov, D. Phase control in the vibrational qubit. *J. Chem. Phys.* **2006**, *125*, No. 024105.

(19) Ospelkaus, S.; Ni, K.-K.; Quéméner, G.; Neyenhuis, B.; Wang, D.; de Miranda, M. H. G.; Bohn, J. L.; Ye, J.; Jin, D. S. Controlling the Hyperfine State of Rovibronic Ground-State Polar Molecules. *Phys. Rev. Lett.* **2010**, *104*, No. 030402.

(20) Blackmore, J. A.; Gregory, P. D.; Bromley, S. L.; Cornish, S. L. Coherent manipulation of the internal state of ultracold $^{87}Rb^{133}Cs$ molecules with multiple microwave fields. *Phys. Chem. Chem. Phys.* **2020**, *22*, 27529−27538.

(21) Asnaashari, K.; Krems, R. V. Quantum annealing with pairs of $^2\Sigma$ molecules as qubits. *Phys. Rev. A* **2022**, *106*, No. 022801.

(22) Nielsen, M. A.; Chuang, I. L. *Quantum Computation and Quantum Information*; 10th Anniversary Edition, Cambridge University Press, 2010.

(23) Lemeshko, M.; Krems, R. V.; Doyle, J. M.; Kais, S. Manipulation of molecules with electromagnetic fields. *Mol. Phys.* **2013**, *111*, 1648−1682.

(24) Gorshkov, A. V.; Manmana, S. R.; Chen, G.; Ye, J.; Demler, E.; Lukin, M. D.; Rey, A. M. Tunable Superfluidity and Quantum Magnetism with Ultracold Polar Molecules. *Phys. Rev. Lett.* **2011**, *107*, No. 115301.

(25) Wall, M. L.; Hazzard, K. R. A.; Rey, A. M. *From Atomic to Mesoscale. The Role of Quantum Coherence in Systems of Various Complexities*; World Scientific, 2015; p 3.

(26) Gorshkov, A. V.; Manmana, S. R.; Chen, G.; Demler, E.; Lukin, M. D.; Rey, A. M. Quantum magnetism with polar alkali-metal dimers. *Phys. Rev. A* **2011**, *84*, No. 033619.

(27) Aldegunde, J.; Rivington, B. A.; Żuchowski, P. S.; Hutson, J. M. Hyperfine energy levels of alkali-metal dimers: Ground-state polar molecules in electric and magnetic fields. *Phys. Rev. A* **2008**, *78*, No. 033434.

(28) Yan, B.; Moses, S. A.; Gadway, B.; Covey, J. P.; Hazzard, K. R. A.; Rey, A. M.; Jin, D. S.; Ye, J. Observation of dipolar spin-exchange interactions with lattice-confined polar molecules. *Nature* **2013**, *501*, 521−525.

(29) Lin, J.; He, J.; Jin, M.; Chen, G.; Wang, D. Seconds-Scale Coherence on Nuclear Spin Transitions of Ultracold Polar Molecules in 3D Optical Lattices. *Phys. Rev. Lett.* **2022**, *128*, No. 223201.

(30) Briegel, H. J.; Raussendorf, R. Persistent Entanglement in Arrays of Interacting Particles. *Phys. Rev. Lett.* **2001**, *86*, 910−913.

(31) Briegel, H. J.; Browne, D. E.; Dür, W.; Raussendorf, R.; Van den Nest, M. Measurement-based quantum computation. *Nat. Phys.* **2009**, *5*, 19−26.

(32) Jones, J. A. Robust Ising gates for practical quantum computation. *Phys. Rev. A* **2003**, *67*, No. 012317.

(33) Ma, J.; Wang, X.; Sun, C. P.; Nori, F. Quantum spin squeezing. *Phys. Rep.* **2011**, *509*, 89−165.

(34) Pezzè, L.; Smerzi, A.; Oberthaler, M. K.; Schmied, R.; Treutlein, P. Quantum metrology with nonclassical states of atomic ensembles. *Rev. Mod. Phys.* **2018**, *90*, No. 035005.

(35) Rost, J. M.; Griffin, J. C.; Friedrich, B.; Herschbach, D. R. Pendular states and spectra of oriented linear molecules. *Phys. Rev. Lett.* **1992**, *68*, 1299−1302.
(36) Bhongale, S. G.; Mathey, L.; Zhao, E.; Yelin, S. F.; Lemeshko, M. Quantum Phases of Quadrupolar Fermi Gases in Optical Lattices. *Phys. Rev. Lett.* **2013**, *110*, No. 155301.
(37) Stone, A. J. *The Theory of Intermolecular Forces*; Oxford University Press, UK, 2013.
(38) Barry, J. F.; McCarron, D. J.; Norrgard, E. B.; Steinecker, M. H.; DeMille, D. Magneto-optical trapping of a diatomic molecule. *Nature* **2014**, *512*, 286−289.
(39) Truppe, S.; Williams, H. J.; Hambach, M.; Caldwell, L.; Fitch, N. J.; Hinds, E. A.; Sauer, B. E.; Tarbutt, M. R. Molecules cooled below the Doppler limit. *Nat. Phys.* **2017**, *13*, 1173.
(40) Anderegg, L.; Augenbraun, B. L.; Bao, Y.; Burchesky, S.; Cheuk, L. W.; Ketterle, W.; Doyle, J. M. Laser cooling of optically trapped molecules. *Nat. Phys.* **2018**, *14*, 890−893.
(41) McCarron, D. J.; Steinecker, M. H.; Zhu, Y.; DeMille, D. Magnetic Trapping of an Ultracold Gas of Polar Molecules. *Phys. Rev. Lett.* **2018**, *121*, No. 013202.
(42) Rvachov, T. M.; Son, H.; Sommer, A. T.; Ebadi, S.; Park, J. J.; Zwierlein, M. W.; Ketterle, W.; Jamison, A. O. Long-Lived Ultracold Molecules with Electric and Magnetic Dipole Moments. *Phys. Rev. Lett.* **2017**, *119*, No. 143001.
(43) Son, H.; Park, J. J.; Ketterle, W.; Jamison, A. O. Collisional cooling of ultracold molecules. *Nature* **2020**, *580*, 197−200.
(44) Ding, S.; Wu, Y.; Finneran, I. A.; Burau, J. J.; Ye, J. Sub-Doppler Cooling and Compressed Trapping of YO Molecules at μK Temperatures. *Phys. Rev. X* **2020**, *10*, No. 021049.
(45) Burau, J. J.; Aggarwal, P.; Mehling, K.; Ye, J. Blue-Detuned Magneto-optical Trap of Molecules. *Phys. Rev. Lett.* **2023**, *130*, No. 193401.
(46) Derevianko, A.; Cannon, C. C. Quantum computing with magnetically interacting atoms. *Phys. Rev. A* **2004**, *70*, No. 062319.
(47) Vargas-Hernández, R. A.; Krems, R. V. Engineering extended Hubbard models with Zeeman excitations of ultracold Dy atoms. *J. Phys. B: At., Mol. Opt. Phys.* **2016**, *49*, No. 235501.
(48) Chomaz, L.; Ferrier-Barbut, I.; Ferlaino, F.; Laburthe-Tolra, B.; Lev, B. L.; Pfau, T. Dipolar physics: a review of experiments with magnetic quantum gases. *Rep. Prog. Phys.* **2022**, *86*, No. 026401.
(49) Stoll, M.; Bakker, J. M.; Steimle, T. C.; Meijer, G.; Peters, A. Cryogenic buffer-gas loading and magnetic trapping of CrH and MnH molecules. *Phys. Rev. A* **2008**, *78*, No. 032707.
(50) Yu, P.; Cheuk, L. W.; Kozyryev, I.; Doyle, J. M. A scalable quantum computing platform using symmetric-top molecules. *New J. Phys.* **2019**, *21*, No. 093049.
(51) Changala, P. B.; Weichman, M. L.; Lee, K. F.; Fermann, M. E.; Ye, J. Rovibrational quantum state resolution of the C_{60} fullerene. *Science* **2019**, *363*, 49−54.
(52) Liu, L. R.; Changala, P. B.; Weichman, M. L.; Liang, Q.; Toscano, J.; Kłos, J.; Kotochigova, S.; Nesbitt, D. J.; Ye, J. Collision-Induced C_{60} Rovibrational Relaxation Probed by State-Resolved Nonlinear Spectroscopy. *PRX Quantum* **2022**, *3*, No. 030332.
(53) Baum, L.; Vilas, N. B.; Hallas, C.; Augenbraun, B. L.; Raval, S.; Mitra, D.; Doyle, J. M. 1D Magneto-Optical Trap of Polyatomic Molecules. *Phys. Rev. Lett.* **2020**, *124*, No. 133201.
(54) Mitra, D.; Vilas, N. B.; Hallas, C.; Anderegg, L.; Augenbraun, B. L.; Baum, L.; Miller, C.; Raval, S.; Doyle, J. M. Direct laser cooling of a symmetric top molecule. *Science* **2020**, *369*, 1366−1369.
(55) Wall, M. L.; Maeda, K.; Carr, L. D. Realizing unconventional quantum magnetism with symmetric top molecules. *New J. Phys.* **2015**, *17*, No. 025001.

https://doi.org/10.1021/acs.jpca.3c02835
J. Phys. Chem. A 2023, 127, 6593−6602